Effect of claystone small-scale characteristics on the variability of micromechanical response and on microcracking modelling

Benoît Pardoen, Pierre Bésuelle, Stefano Dal Pont, Philippe Cosenza, Jacques Desrues

Effect of claystone small-scale characteristics on the variability of micromechanical response and on microcracking modelling

Benoît Pardoen[1,*], Pierre Bésuelle[2], Stefano Dal Pont[2], Philippe Cosenza[3], and Jacques Desrues[2]

[1] Laboratoire de Tribologie et Dynamique des Systèmes (LTDS), Ecole Nationale des Travaux Publics de l'Etat (ENTPE), 69120 Vaulx-en-Velin, France
[*]benoit.pardoen@entpe.fr

[2] Univ. Grenoble Alpes, CNRS, Grenoble INP, 3SR, 38000 Grenoble, France

[3] Institut de Chimie des Milieux et Matériaux de Poitiers (IC2MP), Université de Poitiers, 86000 Poitiers, France

Abstract Argillaceous rocks have a complex and heterogeneous structure at different scales. At the scale of the mineral inclusions embedded in a clay matrix, the deformation generally induces microcracking and material damage. Modelling the latter requires to take into account microscale characteristics and their effect on the micromechanical response. This response can be used in double scale approach to predict material behaviour at larger scale. Thus, heterogeneous microstructures of a claystone are generated with a distribution of morphological properties satisfying experimental observations. The overall microscale material behaviour under solicitation is obtained by numerical homogenisation. Then, the variability of the material response is studied with regard to small-scale characteristics. In terms of deformation and failure, a dominant shear deformation mode and decohesion between grains are observed. The decohesion induces microcracking in the microstructure and strain softening of its overall response.

Keywords: Modelling, Clay rock, Micromechanics, Homogenised response, Microcracking.

1 Introduction

Clayey rocks are considered as host rocks for deep geological repository of nuclear wastes. The role of material microstructure on the mechanical behaviour at macroscopic scale is a crucial issue. Clay rocks have a complex heterogeneous structure over a wide range of scales. For deformation, mechanical damage, and macroscopic failure, the most relevant scale is the one of the mineral inclusions and microcracking, i.e. the micrometric scale (Desbois et al., 2017). In the following, the material behaviour and its characteristics are considered at this scale. The mineralogical properties include grain morphology and mineral phase proportions. Defining realistic microstructure allows to derive the overall microscale behaviour by computational homogenisation. The material behaviour variability is then analysed regarding microstructure variabil-

ity, microstructure size, and grain morphology. Hereafter, the studied clay rock and its microstructure are firstly described. Secondly, the generation of representative numerical microstructures is built from realistic characteristics obtained based on experimental characterisation. Thirdly, the used microscale model is briefly presented. Lastly, the clay rock behaviour is modelled leading to the reproduction of mechanical response, deformation, micro-damage, and microcracking that depend entirely on the microstructure. The behaviour variability is also investigated with regard to microscale properties.

2 Clay rock microstructure

The considered material is the Callovo-Oxfordian claystone (COx) studied by the ANDRA in France for nuclear wastes repository. The COx claystone is a cross-anisotropic, low-permeable, and indurated shale with quasi-horizontal bedding planes. The mineralogical characteristics and the generation of representative microstructures are detailed in this section.

At microscale, the structure of the COx claystone is heterogeneous due to the presence of several mineral types. In the following, the considered small scale is the one of the mineral inclusions and experimental evidences (Yven et al., 2007; Robinet et al., 2012; Cosenza et al., 2015; Armand et al., 2017) are used to represent the claystone microstructure in a realistic manner. The zone of interest is the COx clay-rich unit (located at 490m depth). It is a zone composed of a high clay mineral content in the form of a porous clay matrix which embedded non-porous mineral inclusions (Robinet et al., 2012). Its main mineralogical characteristics are detailed hereunder with average values summarised in Table 1. These values are derived from 2D vertical material sections (SEM and X-ray micro-CT) perpendicular to the bedding planes (Robinet et al. 2012).

- Mineralogical composition: Tectosilicates (mostly quartz) 15-25%, carbonates (mostly calcite) 25-35%, heavy minerals (pyrite) 0-3% and clay minerals 40-60% (Armand et al., 2017).
- Size of mineral inclusions: It ranges from several to a few hundreds of micrometers (Robinet et al., 2012). Quartz grains are larger than carbonates, in average, and pyrite grains are the smallest.
- Morphology of mineral inclusions: In average, carbonate inclusions are more elongated than quartz (2D elongation =1 if round, <<1 if elongated in Table 1 and Fig. 1c). The average preferential orientation is horizontal (0°, Fig. 1d) and thus parallel to the bedding planes.
- Characteristic size: For morphological characteristics, the size and length of a Representative Elementary Volume (REV) are $V_{REV}\approx 0.001 mm^3$ and $L_{REV}\approx 100 \mu m$ (Robinet et al., 2012; Cosenza et al., 2015).

Furthermore, deformation and cracking mechanisms occur at microscale. Potential decohesion mechanisms around mineral inclusions and microcracking within the clay matrix develop in the claystone (Desbois et al., 2017; Bésuelle et al., 2019). Contacts between clay matrix and non-clay inclusions serve as microcrack attractors. Then, intergranular microcracking paths develop through the clay matrix (Desbois et al., 2017).

Table 1 Average mineralogical characteristics of the COx claystone (EST26095)

Minerals	Orientation	Elongation [-]	Mean area [µm²]	Area fraction [%]
Clay matrix	-	-	-	50
Pyrite	-	-	-	2
Calcite	horiz.	0.55	45	30
Quartz	horiz. (variable)	0.64	100	18

From the above mineralogical characteristics, it is possible to generate realistic microstructures. 2D microscale elementary areas (EA) are developed to represent the grains and the failure modes at small scale. Heterogeneous microstructures are generated with periodic random Voronoï tessellation. It allows to define the solid grains, each cell representing an inclusion or a clay grain (see Fig. 1a). The generation method is adapted from van den Eijnden et al. (2017) to enrich the mineralogical characteristics (Pardoen et al., 2020). A variability of the latter is also considered to reproduce the observed distribution of clay and mineral contents, orientation, and elongation. Examples of realistic microstructures of COx claystone are visible in Fig. 1a and Fig. 3a.

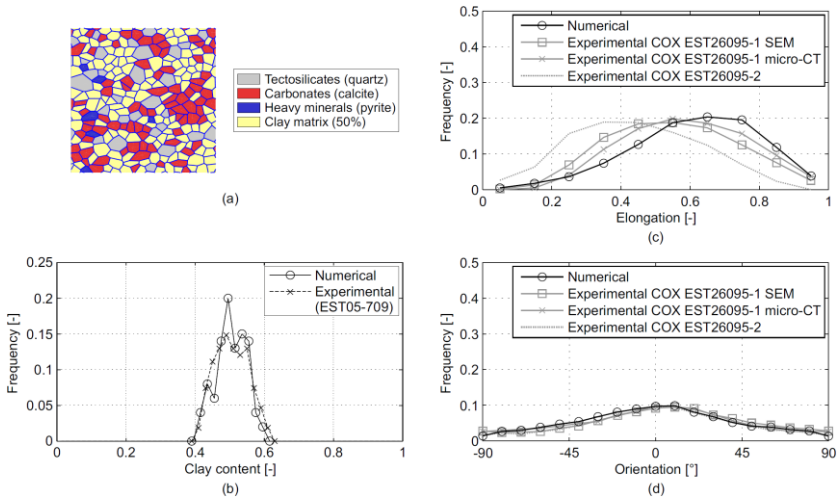

Fig. 1 Representativeness of the microstructures: (a) example of numerical elementary area, (b) distributions of clay content, (c,d) comparison of experimental and numerical morphological characteristics of calcite (Robinet 2008)

As aforementioned, the considered elementary areas are representative of vertical sections perpendicular to the bedding planes. They are numerically dimensionless; however, an artificial characteristic size of L_{EA}=100µm (corresponding to experimental measurements) is assign by choosing the number of grains represented (250 Voronoï cells). The microstructure representativeness and variability are assessed by comparing experimental and numerical morphological characteristics of minerals. The comparison in Fig. 1 is realised on a set of 100 numerical EAs. It highlights the accurate reproduction of clay contents and morphology of inclusions. This reproduction of morphological characteristics together with the consideration of deformation and cracking mechanisms in section 3 lead to a realistic definition of the material microstructure.

3 Microscale model

The microscale model contains the details of the material microstructure and is embedded in a double-scale finite element (FE²) approach (Frey et al., 2013; van den Eijnden et al., 2016, 2017). The overall response of periodic microscopic EA is derived by microscale finite element computation and then used as a homogenised implicit constitutive model at macroscale (by computational homogenisation). The scale transition is realised by enforcing periodic boundary conditions on the 2D microscale model (under plane strain conditions) which result of the macrostrain. Hereafter, the focus is on the microscale model definition and its ability to reproduce the behaviour of clay rock, including the deformation processes at grain scale.

The generated EAs (Fig. 1a) are defined as assemblies of (isotropic linear) elastic deformable continuous solid grains in interaction with cohesive crack models. The latter are damageable cohesive interfaces which permit material softening due to deformation. Thus, the non-linearity of the material behaviour is concentrated at grain contacts. The cohesive laws in both tangential and normal contact directions are given by:

$$c_t = \frac{1}{D_t}(1 - D_t)\frac{\Delta u_t}{\delta_t^c} c_t^{max} \tag{1}$$

$$c_n = \frac{1}{D_n}(1 - D_n)\frac{\Delta u_n}{\delta_n^c} c_n^{max} - \kappa\, \Delta u_n^2 \tag{2}$$

where t and n subscripts correspond to tangential and normal directions, $c_{n/t}$ are interface cohesion forces, $c_{n/t}^{max}$ are maximal cohesion forces, $\Delta u_{n/t}$ are interface relative displacements. Then, $D_{n/t}$ are softening parameters representing the interface degradation state $0 \leq D_{n/t} \leq 1$ (depending on initial degradation states $D_{n/t}^0$ and time history of $\Delta u_{n/t}$), $\delta_{n/t}^c$ are critical relative displacements inducing complete decohesion ($D_{n/t}$=1, $c_{n/t}$=0), and κ is a penalisation term to avoid grain interpenetration ($\kappa >> c_n^{max}$ if Δu_n<0, κ=0 if $\Delta u_n \geq 0$).

Following the above definitions, large deformations may develop at microscale and are mainly concentrated at grain contacts. Potential microcracks are considered at grain interfaces which allows two failure types as observed in the clay rock (Desbois et al., 2017; Bésuelle et al., 2019): decohesion around inclusions (inclusion-clay contacts) and intergranular microcracking within the clay matrix (clay-clay contacts). Grain breakage is not considered. However, numerous possible microcrack paths can develop within the clay matrix. Furthermore, only crack porosity is considered at grain interfaces.

4 Modelling of clay rock behaviour

The micromechanical properties of the heterogeneous EAs are chosen to reproduce the clay rock behaviour (Table 2). Each mineral constituent is assigned linear elastic properties (Ahrens, 1995; Robinet et al., 2012; van den Eijnden et al., 2017) and homogeneous interface properties are assumed (van den Eijnden et al., 2017; Pardoen et al., 2020). The clay rock micromechanical behaviour is analysed through the responses of EAs subjected to loading. A biaxial compression is numerically modelled in 2D plane strain state with a first isotropic confining phase followed by a vertical compression (enforced global homogenised vertical strain ε_1) under constant lateral confining pressure σ_3. The variability of material response and deformation processes under deviatoric solicitation are analysed. Stress-strain deviatoric response curves are detailed in Fig. 2 for σ_3=12MPa. They present the evolution of the global deviatoric stress $q=\sigma_1-\sigma_3$ with the homogenised vertical ε_1 and lateral ε_3 strains of the EAs. Numerical results indicate that the microscale overall response shows some dispersion due to the variability of the microstructures (i.e. variable inclusion positions, mineral contents, and grain morphology).

Table 2 Microscale mechanical parameters

Minerals	ν [-]	E [GPa]		
Clay matrix	0.110	2.3		
Pyrite	0.154	305		
Calcite	0.317	84		
Quartz	0.074	95		
Interfaces	$c_n^{max}\ [MPa]$	$c_t^{max}\ [MPa]$	$D_{n/t}^0\ [-]$	$\delta_{n/t}^c\ [-]$
	1.0	2.5	0.001	0.1

The results in Fig. 2a highlight the response scattering related to the randomness of inclusion positions, morphology, and mineral contents (random EA generation). In Fig. 2b, the mineral contents are fixed with 50% of clay and only the range and the average response curves are detailed. The highlighted variability suggests that the chosen EA size, based on grain morphology, is not sufficient regarding the mechanical response.

The effect of microstructure size is studied for different number of cells in the EAs. 50, 100, and 250 cells lead to mean characteristic lengths of L_{EA} = 50, 70, and 105 µm (Fig. 3a). The other micromechanical parameters are kept from Tables 1-2, with 50% of clay. For each case, the range of response curves (over 10 EAs) is illustrated in Fig. 3b. The variability of the microscale response reduces with increasing size, which mitigates the partial lack of EA representativeness. A number of 250 grains is kept as a compromise between representativeness and computation cost in double-scale framework.

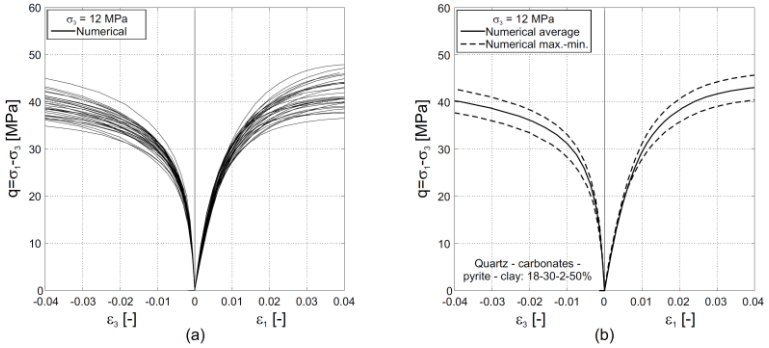

Fig. 2 Microscale response variability to the randomness of EA generation and mineral contents: (a) variable mineral contents (40% to 60% of clay), (b) fixed contents (50% of clay)

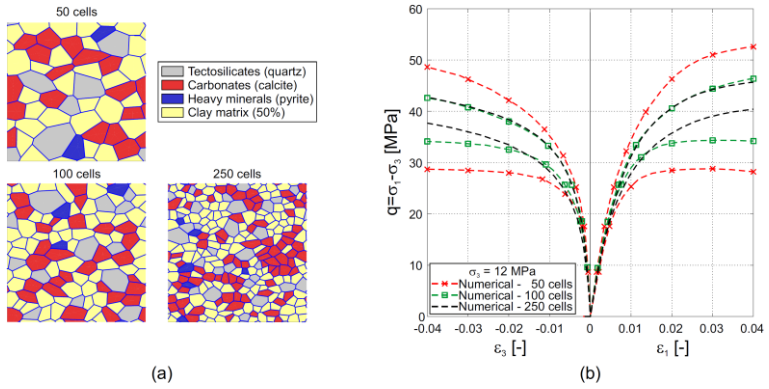

Fig. 3 Microscale response variability to microstructure size: (a) microstructures and (b) range of material response

The deformation at small-scale within the microstructure deserves also to be analysed. One microstructure (numbered [1]) with 60% of clay content is firstly studied to enlighten grain movements and micro-damage of interfaces. The response curve and the small-scale deformation are detailed in Fig. 4a-b [1] (up to ε_1=0.1). A peak deviatoric stress followed by strain softening occurs (Fig. 4a), which is characteristic of dense material failure. The amplitude of material softening depends on the interface properties. Furthermore, microscale deformations are detailed at several stages of the vertical loading (Fig. 4b), before (ε_1=0.01) and after peak stress (ε_1=0.05, 0.1). Cohesion sof-

tening ($D_{n/t}$<1) and complete decohesion ($D_{n/t}$=1) of interfaces (i.e. partially and fully damaged) are indicated by graphical symbols in Fig. 4b. The microstructure deformation remains limited before peak stress. Then, damage increases, coalesces, and forms a microcrack propagating through the entire EA. This induces important grain displacements (mainly sliding, Fig. 4b) and a global softening behaviour of the microstructure (Fig. 4a). Moreover, shearing is the dominant mode of deformation and damage at grain contacts. Only a small proportion of interfaces reaches complete decohesion (Fig. 4b) but contributes significantly to the microscopic localised deformations in the EA.

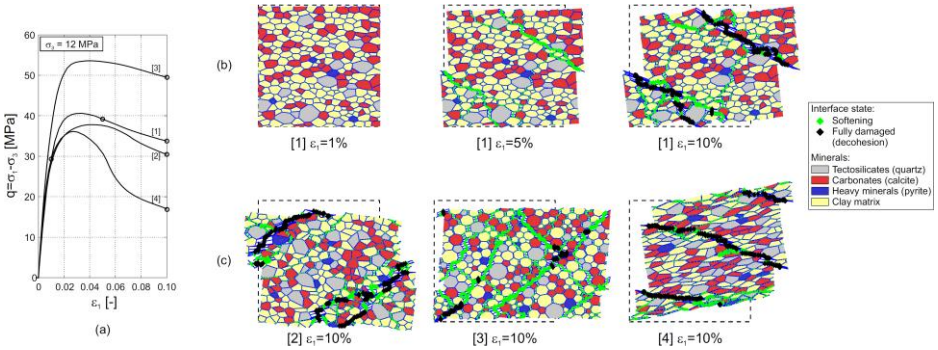

Fig. 4 Microstructural behaviour variability for various types of microstructures: (a) material response, (b) microcrack appearance, (c) microcracking patterns

Let us now consider several microstructures with same size (i.e. same number of cells), 50% of clay content, and identical micromechanical parameters (Table 2). To enlighten the effect of microscale characteristics, the selected EAs represent different degrees of grain elongation, orientation, and angularity. They are presented in deformed state for a global homogenised vertical strain of ε_1=0.1 in Fig. 4c (microstructures [2]-[3]-[4]). The confining pressures is still of σ_3=12MPa as previously and the global response curves are illustrated in Fig. 4a. At ε_1=0.1, all EA responses have reached softening due to grain contact damage. Moreover, the microstructures exhibit various microcracking patterns. The microstructures [1-2] in Fig. 4 have similar grain morphological characteristics but different positions of inclusions and mineral contents. They have similar microcracking patterns but with different locations and inclinations of the micro fault. The other microstructure [3-4] have a different grain morphology. [3] has rounded grains. The results in Fig. 4 show that grain roundness increases the global shear strength (peak deviatoric stress), reduces the softening and damage, and restricts the microcracking appearance. [4] is anisotropic with elongated grains oriented parallel to the claystone bedding planes (horizontal) and a perpendicular (vertical) loading to them. The results show that the elongation does not affect the microcrack orientation, neither the shear strength. Nevertheless, it increases the overall material softening and shearing of the microstructure.

6 Conclusions

The realism of the modelling of clay rock microstructural behaviour is improved by considering heterogeneous microscale characteristics and variability. The representativeness of the small-scale behaviour and the influence of property variability are emphasised. Results indicate that the variability of micromechanical response, small-scale deformations, and microcracking patterns are related to: random positions of inclusions, mineral contents, and grain morphology. The observed variability reduces with the microstructure size. Analysis of micro deformation indicate that shearing mode of deformation is dominant at grain contacts under global deviatoric solicitation. The development of damage in the microstructure is localised and engenders intergranular micro faults, as observed experimentally. This, in turn, leads to microscale strain softening.
Furthermore, the material behaviour is affected by the geometry of potential cracking paths. Finally, the enhancement of microscale behaviour modelling allows new possibilities for realistic upscaled modelling of heterogeneous rocks.

References

Ahrens T (1995) Mineral physics and crystallography: a handbook of physical constants. 354p.

Armand, G., Conil, N., Talandier, J., Seyedi, D.M. (2017). Fundamental aspects of the hydro-mechanical behaviour of Callovo-Oxfordian claystone: From experimental studies to model calibration and validation. *Computers and Geotechnics* 85:277-286.

Bésuelle, P., Andò, E., Stamati, O., Boller, E. (2019). Mesure de champs de déformation dans l'argillite du Callovo-Oxfordien à l'échelle du micron. *In: 3eme journées thématiques des Techniques d'imagerie pour la caractérisation des matériaux et des structures du génie civil*, pp 1-2.

Cosenza, P., Prêt, D., Giraud, A., and Hedan, S. (2015). Effect of the local clay distribution on the effective elastic properties of shales. *Mechanics of Materials* 84,55-74.

Desbois, G., Höhne, N., Urai, J.L., Bésuelle, P., Viggiani, G. (2017). Deformation in cemented mudrock (Callovo-Oxfordian Clay) by microcracking, granular flow and phyllosilicate plasticity: insights from triaxial deformation, broad ion beam polishing and scanning electron microscopy. *Solid Earth* 8(2):291-305.

Frey, J., Chambon, R., Dascalu, C. (2013). A two-scale poromechanical model for cohesive rocks. *Acta Geotechnica*. 8(2):107–124.

Pardoen, B., Bésuelle, P., Dal Pont, S., Cosenza, P., and Desrues, J. (2020). Accounting for small-scale heterogeneity and variability of clay rock in homogenised numerical micromechanical response and microcracking. *Rock Mechanics and Rock Engineering*, under review.

Robinet, J.C., Sardini, P., Coelho, D., Parneix, J.C., Prêt, D., Sammartino, S., Boller, E., and Altmann, S. (2012). Effects of mineral distribution at mesoscopic scale on solute diffusion in a clay-rich rock: Example of the Callovo-Oxfordian mudstone (Bure, France). *Water Resources Research* 48(5).

van den Eijnden, A., Bésuelle, P., Chambon, R., Collin, F. (2016). A FE^2 modelling approach to hydromechanical coupling in cracking-induced localization problems. *International Journal of Solids and Structures* 97-98:475-488.

van den Eijnden, A., Bésuelle, P., Collin, F., Chambon, R., Desrues, J. (2017). Modeling the strain localization around an underground gallery with a hydro-mechanical double scale model; effect of anisotropy. *Computers and Geotechnics* 85:384-400.

Yven, B., Sammartino, S., Geraud, Y., Homand, F., Villieras, F. (2007). Mineralogy, texture and porosity of Callovo-Oxfordian argillites of the Meuse/Haute-Marne region (eastern Paris Basin). *Bulletin de la Societe Geologique de France* 178:73-90.